Computing the effects of YORP on the spin rate distribution of the NEO population

A. Rossi, F. Marzari, D.J. Scheeres

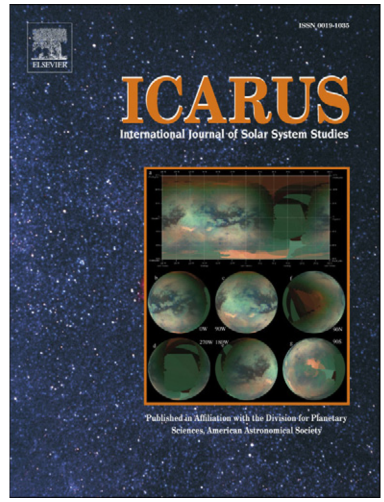

Computing the effects of YORP on the spin rate distribution of the NEO population

A. Rossi, F. Marzari, D.J. Scheeres

PII: S0019-1035(09)00110-9
DOI: 10.1016/j.icarus.2009.02.030
Reference: YICAR 8954

To appear in: *Icarus*

Received date: 28 April 2008
Revised date: 18 February 2009
Accepted date: 25 February 2009

Computing the effects of YORP on the spin rate distribution of the NEO population

A. Rossi
ISTI-CNR, CNR - Area della Ricerca di Pisa, 56124 Pisa, Italy
E-mail: Alessandro.Rossi@isti.cnr.it

F. Marzari
Dipartimento di Fisica, Università di Padova, 35131 Padova, Italy
E-mail: francesco.marzari@pd.infn.it
D. J. Scheeres
Department of Aerospace Engineering Sciences,
The University of Colorado, Boulder, Colorado 80309-0429, USA
E-mail: scheeres@colorado.edu

March 13, 2009

Please, send editorial communications and proofs to:
Alessandro Rossi
ISTI–CNR
CNR - Area della Ricerca di Pisa
Via Moruzzi, 1
56124 Pisa, Italy
Tel: 39-050-3152 953
Fax: 39-050-3152 040
E–mail: Alessandro.Rossi@isti.cnr.it

Manuscript pages: 29

Figures: 5

Running title: Effects of YORP on the NEOs spin rate distribution

Keywords: ASTEROIDS, ROTATION; ROTATIONAL DYNAMICS; YORP.

Abstract

The overall change of NEO spin rate due to planetary encounters and YORP is evaluated by using a Monte Carlo model. A large sample of test objects mimicking a source population is evolved over a timescale comparable with the solar system age until they reach a steady state spin distribution that should reproduce the current NEO distribution. The spin change due to YORP is computed for each body according to a simplified model based on Scheeres (2007a).

The steady state cumulative distribution of NEO spin rates obtained from our simulation nicely reproduces the observed one, once our results are biased to match the diameter distribution of the sample of objects included in the observational database. The excellent agreement strongly suggests that YORP is responsible for the concentration of spin at low rotation rates. In fact, in the absence of YORP the steady state population significantly deviates from the observed one. The spin evolution due to YORP is also so rapid for NEOs that the initial rotation rate distribution of any source population is quickly relaxed to that of the observed population. This has profound consequences for the study of NEO origin since we cannot trace the sources of NEOs from their rotation rate only.

1 Introduction

It is widely believed that the NEO population is constantly replenished by new bodies traveling from their source regions via various dynamical pathways linked to orbital resonances. Most NEOs possibly come from the Main Belt following an asteroidal breakup event. The ejected fragments either end up directly in a resonance and are driven to the terrestrial planet region in a few million years (Gladman et al. 2000, Bottke et al,. 2002) or they evolve under the influence of the Yarkovsky effect and enter the resonances at a subsequent time (Farinella and Vokrouhlický, 1999) contributing to a steady flux. A minor fraction of the NEO population comes from the comet reservoirs, the Kuiper Belt and the Oort cloud (Binzel et al., 1992; Demeo and Binzel, 2008).

At first sight, having such a selection of samples from the Main Belt within our reach appears to be scientifically convenient and can be used to further our knowledge on the nature and origin of minor bodies. NEOs can be more easily studied with observational methods (including radar) and targeted by space missions providing detailed information about their surface properties, shapes and rotation rates. However, the evolution of an NEO during the period where they live in planet crossing orbits, prior to striking either the sun or a planet, may substantially alter their present shapes and rotation rates. These last properties are tightly related since a significant spin up close to the rotational break–up limit (Pravec and Harris, 2000) can lead to a shape change, mass shedding or even fission and binary formation (Scheeres et al. 2007, Scheeres 2007b).

Two major mechanisms are suspected to alter the rotation rates and states of NEOs once they get into planet crossing orbits: close encounters with the planets and YORP. In a recent paper (Scheeres et al. 2004; hereinafter paper I) we modeled the statistical effect of planetary flybys on the spin rate of NEOs with a Monte Carlo numerical approach. We showed that the cumulative effect of planet encounters spin up the NEO population on average, increasing the fraction of bodies close to the disruption limit. In addition, the slow rotation tail of the spin distribution is increased to longer periods accounting for some of the noted excess in slow rotators among the NEOs (Pravec et al., 2008). According to Scheeres et al. (2005) the effects of a close encounter on the rotation rate of NEO asteroid Apophis (2004 MN4) will be measurable using groundbased telescopes during its Earth flyby in 2029.

The second mechanism believed to alter the way NEOs and, in general, any small body in the inner regions of the Solar System rotate is YORP (Rubincam 2000). The YORP effect is due to the reflection and reemission of light by an irregularly shaped asteroid and leads to a net thermal torque acting on that body. YORP is known to have relevant implications in the history of Main Belt asteroids as it can explain the "Slivan states" (Slivan et al. 2003) within the Koronis family by affecting not only the rotation rate but also causing a progressive tilt of the obliquity toward a specific value (Rubincam 2000, Bottke et al. 2002, Vokrouhlický and Capek 2002). It can also account for the excess of slow and fast rotators observed among small asteroids (Pravec and Harris 2000, Pravec et al. 2002, Pravec et al. 2008). Since YORP is proportional to the inverse square of distance from the sun, as expected for a force related to solar irradiation, for NEOs it becomes very influential. Recently its effect was directly measured via radar and optical observations of the ~ 100 m size near–Earth asteroid (54509) 2000 PH5 and (1862) Apollo. Lowry et al. (2007), Taylor et al. (2007) and Kaasalainen et al. (2007) found continuously increasing spin rates for these asteroids consistent with the theoretical expectations of YORP.

A way to estimate the overall change of the NEO spin rate due to planetary encounters and YORP is to compute the steady state spin distribution of a large sample of objects. The modeling must include a reasonable description of the NEO dynamics and of the sink mechanism since they both appear as relevant aspects in the computation of the spin perturbing torques.

We revisited our Monte Carlo model described in Paper I by including the YORP–driven evolution of the spin axis as described in Scheeres (2007a). We start the model with an initial distribution of a large number of NEOs with a Maxwellian spin rate distribution expected for small collisional fragments in the Main Belt. The population is then evolved over a long period of time by updating the spin rate with changes due to both close encounters and YORP. When we reach a stationary distribution, we compare it with observational data (Pravec et al. 2008). In this way we can quantitatively estimate the number of bodies accelerated to a fast or slow rotation state and compare our predictions with observations. We can also evaluate the relative relevance of the two mechanisms affecting the spin rate. A reverse process can also be adopted with the parameters of the YORP model being finely tuned in order to reproduce the observations, allowing deeper insight into the theoretical modeling.

In Sect. 2 we describe the YORP theory we use in the Monte Carlo approach. In Sect. 3 we briefly recall the main features of the code and the modifications we performed to include YORP. Sect. 4 is devoted to the description of the results while in Sect. 5 we comment and discuss the findings.

2 YORP: the model

The YORP effect acts on both the spin rate and obliquity of an asteroid. It was first proposed to be important for asteroids in Rubincam (2000), and was later verified for two different asteroids in 2007 (Lowry et al. 2007 and Kaasalainen et al. 2007). It has been studied via numerical and semi-analytical approaches in a variety of papers (Vokrouhlický and Capek 2002, Scheeres 2007a, Nesvorný and Vokrouhlický 2007, Scheeres and Mirrahimi 2008). In our model we use the theory as outlined in Scheeres (2007a). In that paper the torque acting on an asteroid from the YORP effect is decomposed into a Fourier Series, where the coefficients of these series can be derived from a general shape model for an asteroid. With this decomposition, it then becomes possible to evaluate the averaged dynamical evolution of an asteroid's spin state, and relate it to a few simple constants. Such an analysis was performed in Scheeres (2007a) and applied to a number of asteroid shape models. It was found that the shape-derived YORP coefficients for this collection of asteroids, when properly normalized by their size and density, were distributed randomly within a certain interval of values.

Denote this non-dimensional YORP coefficient as C_Y, where $-0.025 \leq C_Y \leq 0.025$, inferred from Table 4 in Scheeres (2007a). We note that, based on values taken from (Kaasalainen et al. 2007 and Taylor et al. 2007), the estimated values of the YORP coefficient coefficient for the asteroids Apollo and YORP are 0.022 and 0.005, respectively. As will be detailed later, in the simulation code the value of C_Y is drawn randomly for every new asteroid, independent of its size and other quantities. To convert this non-dimensional number to an actual acceleration we require values for the asteroid's mean radius, density, and orbit. The rotational acceleration for the body is then computed as:

$$\dot{\omega} = \frac{BG_1 r}{a^2\sqrt{1-e^2}M} C_Y \tag{1}$$

where B is a Lambertian scattering coefficient, usually taken equal to 2/3 (e.g., McInnes 1999), $G_1 \sim 1 \times 10^{14}$ kg km/s^2 is the solar radiation constant, a is the asteroid heliocentric orbit semi-major axis (km), e is the asteroid heliocentric eccentricity, r is the asteroid mean radius and M is the asteroid mass, computed from an assumed density and mean radius. Thus, given the non-dimensional coefficient, we note the proper $1/r^2$ dependence on size and $1/A^2$ dependence on orbit. The coefficient C_Y contains combined information on the asteroid's shape and moment of inertia.

To realistically evolve single bodies it is necessary to evaluate their obliquity and rotation rate equations as a function of time for a specified shape model. As we are only concerned with the statistical distribution of the rotation rates, however, we consider a simplified model for YORP evolution. In our approximation we ignore the obliquity dynamics and allow the rotation rate acceleration to change at a uniform rate, but based on a randomly chosen YORP coefficient. We argue that, although the individual dynamical evolutions of these spin states will not be realistic, the averaged evolution will be correct to first order. This is mainly due to the fact that most obliquity evolutions of asteroids reinforce the spin-down or spin-up of asteroids. There are some situations where an asteroid's spin state can approach a limit cycle, however these cases should be more rare (Scheeres and Mirrahimi 2008).

In the evolution of the spin rate, we also note the sensitivity of the YORP effect to the shape of an asteroid, as documented in Scheeres et al. (2007). Thus, when an asteroid approaches the surface disruption rate we suppose that its shape can distort, due to the reconfiguration of boulders or components of the asteroid as theorized in Scheeres et al. (2007) and discussed in more detail in Scheeres (2008). In this way we assume that a larger asteroid spun to its disruption rate can have its shape shifted until it is "reflected" by obtaining a negative value of its YORP coefficient and commence a period of deceleration. For the opposite situation, when an asteroid's spin rate approaches zero, we assume that YORP supplies a nearly constant torque that acts to spin the body up in the opposite direction (see

Vokrouhlický et al. 2007). Here we do not assume any change to the body's shape or YORP coefficient during that transition.

Our current model does not include the formation of binary objects by rotational fission due to YORP (Scheeres 2008), even though this is one of the prime candidates for the formation of binary asteroid systems (Walsh and Richardson 2008). Our neglect is justified in light of current best estimates of the lifetimes of binary asteroid systems, found in (Cuk and Burns 2005), which are short in relation to our Monte Carlo time-step. Modeling of this effect is of interest, however, and will be included in future analyses once additional research into these effects are completed.

3 The Monte Carlo numerical model

In this Section we describe the Monte Carlo numerical code used to model the evolution of the NEO spin rates. Some features are already extensively described in Paper I and they will be only briefly summarized here. We will concentrate on the new algorithms in the code developed to account for the YORP torque on asteroids.

3.1 The model NEO population

We start each simulation with a population made of 2×10^4 fictitious NEOs modeled as triaxial ellipsoids endowed with semi–axis a, b, c and effective diameter $D = 2a(bc/a^2)^{1/3}$. The size distribution adopted for the diameters is that given by the Spaceguard Survey (Morrison, 1992) while the axis ratios are computed with a Monte Carlo technique based on the shape distributions given in Giblin et al. (1998). This distribution is the outcome of a series of catastrophic disruption experiments and is well suited to describe fragments of asteroid collisions in the Main Belt, the major source of NEOs. For each body of the ensemble we compute a starting rotation rate from a Maxwellian frequency distribution function (Fulchignoni et al., 1995; Donnison and Wiper, 1999) with a mean period that is a free parameter of the code depending on the source of NEOs. It is now well known (Pravec *et al.*, 2002) that the actual distribution of the rotation rates is best fitted by a sum of two distributions, a fully evolved one for the small sizes and an unevolved one for the large sizes. Here a single Maxwellian is chosen to represent a starting "unevolved" distribution.

3.2 Statistical approach to the dynamics of NEOs

A unique feature of the revised code is the ability to model, in a statistical way and with a few simplifying assumptions, the dynamical behavior of NEOs. This is needed to account for the limited NEO lifetime due to impacting the sun or a planet, or escaping from the solar system. Moreover, we also need to describe in broad terms the time evolution of the most important orbital elements of the fictitious NEO, i.e. semimajor axis a and eccentricity e since these are relevant parameters in the computation of the YORP torque according to Eq. 1. In the task of modeling the dynamical evolution of our fictitious NEO ensemble we are assisted by the chaotic nature of the NEO motion triggered by the frequent close encounters with the terrestrial planets. As shown by numerical computations of NEO trajectories (Milani et al. 1990, Gladman et al. 2000), the evolution of both a and e is similar to a random walk characterized by a progressively decreasing perihelion distance. With this in mind, we conceived an algorithm that assigns to each body in the ensemble an initial pair of (a, e) values selected randomly from the observed distribution of the NEO orbital elements (taken from the NEODYS site, at *newton.dm.unipi.it/neodys/*). After each timestep, a number of bodies exit the ensemble according to an exponential law $N(dt) = N_0(1 - e^{-dt/\tau})$ where N_0 is the initial number of objects, $\tau = 14.5$ Myr is the half–life given in Gladman et al. (2000) and dt is the timestep of the simulation. This is intended to model the sink mechanism. The dismissed bodies are selected randomly among those having the lower perihelion distance $q = a(1 - e)$. To the new bodies, introduced in the ensemble to keep the total number of the population N_0 constant, a new pair of (a, e) values in the outer range of the q distribution is assigned. At the same time, all the remaining bodies are scaled along the q distribution following their aging. After a few timesteps, the fictitious NEO population relaxes to an orbital element distribution reproducing the observed one with the older bodies having lower values of q. This algorithm is substantially different from that proposed in Paper I and it allows not only a reasonable treatment of YORP but also a more reliable modeling of close encounter effects on the rotation rate. As an example, in Fig. 1 the time evolution of the perihelion distance q of 3 objects within our sample population is shown. Older bodies within the simulation are those that will have a higher chance to be removed from the population. Those whose orbit intersects either that of the Earth or Venus are candidates for impacting the planets and being removed before their perihelion reaches the sun.

3.3 Evolution of the rotation rate

The change in the rotational frequency of a body, $\dot{\omega}$, is computed during each timestep dt by taking into account gravitational and non-gravitational interactions. We first compute $\Delta\omega_C$, the variation due to close encounters, for those bodies having flybys with the planets. They are selected randomly among the population and their total number is computed by scaling the collision probability at different distances, r, from each planet by r^2, including the effects of gravitational focusing. The assumed value for the NEO–planet relative velocity (the velocity at infinity) is 16.16 km s^{-1} for the Earth and 22.00 km s^{-1} for Venus (Scheeres et al. 2004) while the geometry of the approach is randomly chosen.

The spin evolution due to YORP, $\dot{\omega}_Y$, is computed for each body according to the following procedure. All the members of the ensemble have a given value of the YORP coefficient C_Y drawn randomly at the beginning of the simulation in the range $[-2.5 \times 10^{-2} : 2.5 \times 10^{-2}]$ (see Sec. 2). For each object, the ratio of the effective radius over the total mass is computed as:

$$\frac{r}{M} = \frac{3}{4} \frac{(abc)^{-\frac{2}{3}}}{\pi \varrho}$$

where a, b and c are the semiaxes of the ellipsoid in km and ϱ is the density in kg/km^3. The YORP acceleration is computed following Eq. 1:

$$\dot{\omega}_Y = \frac{2}{3} 10^{14} C_Y \frac{r}{M} \frac{1}{A^2 \sqrt{1-e^2}}$$

where the 2/3 factor is the assumed Lambertian emission coefficient for the asteroid surface. This equation assumes that the YORP torque is due to thermally radiated heat only. The 10^{14} factor is due to the solar constant in kg km s^{-2}. From the maximum rotation rate of each object (defined later) we can compute a characteristic YORP time, i.e. the time it takes to decelerate from its maximum rate to zero:

$$T_Y = \frac{\omega_M}{|\dot{\omega}_Y|}$$

After any timestep, ω is linearly updated as:

$$\omega = \omega_0 + t\,\dot{\omega}_Y$$

where ω_0 is the value before the timestep.

While YORP exerts a continuous torque on the rotational frequency, $\Delta\omega_C$ is by nature an impulsive effect. Therefore, if a planetary encounter is recorded during a timestep, we apply YORP up to the moment of the encounter. After the encounter the code calculates a new spin state and, if the body survives, YORP is applied again till the end of the timestep. In case of multiple encounters within the same time step, the procedure is repeated. If the object is disrupted by the encounter a new one is drawn from the distribution.

According to the model discussed in Sec. 2, the rotation rate has boundaries within which it evolves because of YORP and encounters. The continuous spin up for positive values of C_Y would lead a body to a very high rotation rate. For rubble–piles we set an upper threshold limit $\omega = \omega_M$ given by the rotational disruption limit. NEOs smaller than a given diameter D (selected as an input parameter) are instead considered monolithic bodies and are not allowed to breakup, so their maximum spin rate before reversing the rotation rate is set as an input variable (the default value, comprising most of the observed NEO, is set to 120 d^{-1}). The minimum value of the spin rate is set to $\omega = 0$. Since we do not have prescriptions from the theory developed in Sec. 2 on how the rotation evolves near these limiting values, we adopt an approximation similar to that described in Pravec et al. (2008). For a despinning body we assume that the rotation, after reaching $\omega = 0$, smoothly restarts in the opposite sense. This is obtained in the code by changing, at the end of the timestep, the sign of the coefficient C_Y becoming now positive. A more realistic modeling should include a period of chaotic tumbling lasting until internal dissipation drives the body back to Short Axis Mode rotation (Burns and Safronov 1979; Harris 1994; Vokrouhlický et al. 2007). However, it is beyond the scope of our statistical approach to estimate the period of time spent tumbling or to model how dissipative effects alter the rotation state.

When a body is spun up to $\omega = \omega_M$ it may undergo reshaping and mass shedding. As described above, we neglect the creation of binary asteroid systems in this version of the code, relying on the predicted short lifetimes of these systems. In the numerical code we assume some reshaping takes place and model the event again by changing the sign of C_Y but keeping the same absolute value (variations of this are considered later). As a consequence, the direction of the YORP evolution is reversed, the body despins ($\dot{\omega} < 0$) and a new YORP cycle starts. Following this strategy, each fictitious NEO may have many YORP cycles before exiting the population. In Fig. 2 we show the histogram of the predicted timescale of YORP cycles within our ensemble. The peak of the distribution is around $\sim 10^5$ yr leading to an estimated number of approximately 150 YORP cycles during the average lifetime of a NEO at the population steady state. Note that the YORP cycles are in most cases shorter than our time step which is 1 Myr. However, we keep track of every cycle an object undergoes and at the end of the timestep it is placed within the correct location along a cycle.

It is noteworthy that the cycle lifetime we estimate on the basis of the theory outlined in Scheeres (2007a) is significantly shorter than the doubling/halting time t_d reported in Pravec et al. (2008) for small Main Belt and Mars Crosser asteroids. Even after scaling for the semimajor axis and size dependence, the discrepancy is still larger by at least a factor 10. We note that the values we use are based on real asteroid shapes and are consistent with the two asteroids which have had their YORP acceleration rate measured.

Note that even if at a first approximation we assume that YORP cannot lead to disruption, close encounters can. A flyby relatively close to a planet can produce an abrupt spin up to a rate where self–gravity cannot hold it together, in particular if the body is a rubble pile. As seen from the simulations in Sec. 4, YORP significantly increases the chance of these events by constantly keeping a fraction of the NEO population close to ω_M. We should note that the theory does indicate that YORP can cause an asteroid to disrupt, as detailed in Scheeres (2007b). Inclusion of a model for binary formation and evolution is of interest for future refinements of this simulation model.

4 Results of the simulations

4.1 Default Case

The introduction of YORP into our Monte Carlo model is highly successful in reproducing the observed population, in particular the excess of slow rotators. We have started a simulation with an initial population of NEO precursors distributed according to a Maxwellian distribution with $\sigma = 2.361$. This choice gives an average rotation period of 6.37 hr typical of fast rotators in the Main Belt, supposedly the source of our NEO model population. The density of the bodies in the sample is set to 2.5 g cm^{-3}. Objects with diameter larger than 250 m are considered as rubble-piles while smaller objects are considered monolithic. The major difference between monolithic bodies and rubble piles is in the maximum spin rate achievable prior to rotational disruption (see previous section).

After some hundred million years the model NEO population reaches a steady state spin distribution which should match the present distribution. However, our distribution is an un–biased sample of NEOs, complete down to small diameters. To compare our steady state spin distribution with the dataset of NEO spin rates from Pravec et al. (2008) we have to artificially bias our model population to reproduce the size distribution of the observational dataset. This can be performed by dividing the diameter range in a series of logarithmic size bins. In each bin we compute the number of observed NEOs and we randomly select an equal number of representative bodies from our sample population (which is by far more numerous). We use the spin rate of these representative bodies to build up the biased model population that can be compared to the observed one in terms of cumulative distribution.

In Fig. 3 we compare the normalized cumulative spin rate distribution of our model population (biased and unbiased) with that of Pravec et al. (2008). The excess of slow rotators with spin rates $\omega < 1$ day^{-1} in the observed distribution is very well reproduced by our biased distribution.

The results shown in Fig. 3 strongly suggests that YORP is mostly responsible for the concentration of spin at low rotation rates. This is confirmed by Fig. 4 where we compare the spin distribution of the steady state model population with and without the YORP effect. It is noticeable that the model population in absence of YORP significantly deviates from that with YORP which, once de–biased, fits the observed distribution very well. The YORP evolution also acts so rapidly that the initial rotation rate distribution of the source population quickly relaxes to that of the observed population. This has profound consequences on the study of NEO origins since we cannot trace the sources of NEOs from their rotation rate only. In Fig. 5 we compare the cumulative distribution of spins for two model steady state NEO populations started with different initial values of σ. The fast rotator population corresponds to our nominal case with initial $\sigma = 2.361$ while the slow rotators have a value of $\sigma = 0.548$ corresponding to an average initial period of 27.46 hr. We notice only little differences between the two evolved populations confirming that YORP is very effective in re–shaping the rotation rate distribution to a common relaxed one. Even if a significant percentage of NEOs were extinct or dormant comets (2–10 % according to Bottke et al. 2002) the YORP cycle would have erased any record of their initial spin rate on a short timescale.

4.2 Sensitivity Analysis

To quantify the sensitivity of our results to our default model we considered a few modifications to the way in which we choose the YORP coefficient C_Y and the way we model what happens when a rubble pile asteroid reaches its maximum spin rate. As stated above, as a default the YORP coefficients C_Y are drawn from a uniform distribution, within a specified range. An additional set of simulations were then performed drawing C_Y from a Gaussian distribution of the form:

$$f(C_Y) = \frac{1}{\sqrt(2\pi\sigma)\exp\left(-0.5{C_Y}^2/\sigma^2\right)}$$

The values of σ clearly trigger the strength of the YORP effect on the overall asteroid population. Several simulations were performed assuming 4 different values of σ: 2.5×10^{-2}, 1.25×10^{-2}, 0.83×10^{-2}, 0.62×10^{-2} (recall that for our uniformly distributed C_Y the maximum absolute value allowed was 2.5×10^{-2}). Fig. 6 shows the comparison between the default case of Fig. 3 (solid line) and the case with Gaussian drawn C_Y, with $\sigma = 1.25 \times 10^{-2}$. The linear behaviour in the mid spin rate range persists but there is an improved matching with the observations at the slow end of the distribution. A more physical distribution of C_Y therefore still improves the model performance. The other three cases with different σ values give lower quality matching with the observed distribution and are not shown here.

Another possible improvement to the default treatment of the YORP effect was tested. As described in the previous Section, it is assumed that, whenever an object reaches the maximum allowed spin rate, the sign of C_Y is changed and a phase of deceleration of the spin rate starts at this point. This assumes that some reshaping is taking place in the object. It can be argued that this reshaping may also lead to a change of the absolute value of C_Y. This possibility was also tested and Fig. 7 shows the comparison between the default case of Fig. 3 (solid line) and the case where both the absolute value and the sign of C_Y are changed each time an object is spun up to $\omega = \omega_M$. Again the behaviour at the mid range and at the high end of the spin rate distribution is not significantly altered, while a noticeable change happens at the slow tail of the distribution, with the creation of a significant excess of slow rotators. Finally, Fig. 8 combines the two variations just described. This Figure shows the results of a simulation where the values C_Y are drawn from a Gaussian distribution with $\sigma = 0.83 \times 10^{-2}$ (note that in Fig. 6 $\sigma = 1.25 \times 10^{-2}$) and both the absolute value and the sign of C_Y are changed each time an object is spun up to $\omega = \omega_M$. We note that as modeling assumptions are changed, slight changes in parameter values allow us to fit the observed population. This confirms that our results are robust and that the comparison to the observed data may lead to some insight on the distribution and evlution of the coefficients C_Y in the NEO population.

4.3 Analytical Model

If we assume that the YORP effect dominates the spin rate of the smaller bodies, we can also construct an analytical prediction of their expected spin-rate distribution. We note that under our model the ensemble values of spin rate will vary uniformly between their maximum rotation rate ω_M and their minimum rate $-\omega_M$. Thus, we can take as the expected probability distribution function for the YORP dominated asteroids a uniform distribution

$$f(\omega) = \frac{1}{2\omega_M}$$

We note that under this distribution the true average value of rotation rate is zero, although this is not relevant to our observations, as we generally only see the magnitude of the spin rate, $|\omega|$.

In Harris (2002) the distribution of asteroid spin rates was considered, using the observed population as data. One of the important conclusions of that paper was that the cumulative distribution for spin rates was linear in the rotation rate, whereas collision theory predicts a distribution proportional to rotation rate cubed. It is simple to recover this result with the above distribution, consistent with the YORP effect. The cumulative probability that an asteroid spin rate is less than a certain value is computed as

$$P(|\omega| \leq \omega') = \int_{-\omega'}^{\omega'} f(\omega) d\omega$$

which can be immediately integrated to find $P(|\omega| \leq \omega') = \frac{\omega'}{\omega_M}$. The cumulative number of asteroids expected to rotate at a rate less than ω' are then the total number of the population multiplied by the cumulative probability, or $N_{Tot}\frac{\omega'}{\omega_M}$. This immediately recovers the linear distribution found in Harris (2002) and Pravec et al. (2008). For more realistic models of the YORP effect and of asteroids, one must consider unique maximum rotation rates for each body and the possibility of a more complex rotation rate evolution at slow spin rates. However, these should be corrections to this distribution. Another important effect is that at slow rotation rates the asteroid is more susceptible to having its spin rate modified by a distant flyby of a planet, which would change the statistics of the slowest rotators. This effect is naturally included in our simulation and may be the cause of the deviation of spin rates from the linear distribution in the slowest spin rates, as seen in Fig. 3 and as noted in Pravec et al. (2008).

5 Discussion and conclusions

With an updated model including both gravitational interaction with the terrestrial planets and the YORP effect, a statistical evolution of the NEO population rotation rate was studied. The new model proves to be very successful in reproducing the observed cumulative distribution of the NEO rotation rates. Starting from a simple Maxwellian distribution, the population of fast and slow rotators observed within the available NEO database is obtained. As explained in Sec. 4, in order to reproduce the observed spin rate distribution it is necessary to bias our simulation results with the diameter distribution from the observational sample of Pravec et al. (2008).

Our simulations show that YORP is the dominant mechanism among NEOs in shaping their spin distribution. The outcomes of models where YORP was switched off deviate significantly from the NEO observed spin distribution. Planetary encounters alone are not effective enough in reproducing the NEO distribution. In addition, since the output of our numerical simulations is an un–biased spin distribution, we can infer from Fig. 3 **and Figs. 6–8** that the real distribution of the NEO spin rate should present an even larger excess of very slow rotators. This is a direct consequence of the fast spin evolution due to YORP. At the same time, we predict that very fast rotators might be oversampled by current observations.

Another important conclusion, suggested by Fig. 5, is that the strong influence of YORP completely erases any reference to the original source population from the observed steady state distribution of the spin rate. This has profound consequences on the study of NEO origins since we cannot trace the sources of NEOs from their rotation rate only.

As pointed out in several points in the text, some of the assumptions of our model compares to those of a simple analytical model developed independently by Pravec et al. (2008) to study the population of small (¡ 15 km) main belt asteroids. Differently from Pravec et al. (2008), our simulation is a true Monte Carlo code, incorporating other effects (such as, e.g., migration of asteroids orbit and planetary flybys) beyond YORP. As noted before for our model, Pravec et al. (2008) also clearly identify YORP as the main driving mechanism for the evolution of the small main belt asteroids and note how the initial distribution of their spin rate has been erased. The Pravec et al. (2008) model recovers the flat, linear distribution of spin rates (as in our analytical derivation), but no attempt is made to match the observed population at the high and low ends of the distribution. The noted excess of slow rotators is heuristically reproduced by reducing the value of the YORP coefficient C, whenever a slow spin rate is reached. On the other hand our model uses YORP coefficients that are drawn from actual bodies and considers different statistical distributions for these coefficients, without any ad-hoc assumption to match the observed distribution in the NEA case.

Further analysis with the improved model described in this paper will include sensitivity of the results to some of the model parameters, for example the rubble-pile vs. monolith dimension threshold, object density, etc. Moreover, in this framework, an analysis of the binary creation rate driven by YORP spin up will be performed, following Scheeres (2007b).

Acknowledgments

DJS acknowledges support by NASA's Planetary Geology and Geophysics Program.

References

Binzel, R.P., S. Xu, S.J. Bus, and E. Bowell 1992. Origins for the near-earth asteroids. *Science* **257**, 779–782.

Bottke, W. F., A. Morbidelli, R. Jedicke, J.M. Petit, H. Levison, P. Michel, and T.S. Metcalfe 2002. Debiased Orbital and Absolute Magnitude Distribution of the Near-Earth Objects. *Icarus* **156**, 399–433.

Burns J.A., and V.S. Safronov 1973. Asteroid nutation angles. *Mon.*

Not. R. Astron. Soc. **165**, 403-411.

Cuk, M. and J.A. Burns. 2005. "Effects of thermal radiation on the dynamics of binary NEAs," *Icarus* 176(2): 418-431.

Demeo, F. and Binzel, R.P. 2008, Comets in the near-Earth object population *Icarus* **194**, 436–449.

Donnison, J. R., and M.P. Wiper 1999. Bayesian statistical analysis of asteroid rotation rates. *Mon. Not. R. Astron. Soc.* **302**, 75–80.

Farinella, P. and Vokrouhlický, D. 1999. Semimajor axis mobility of asteroidal fragments, *Science*, **283**, 1507-1510.

Fulchignoni, M., M.A. Barucci, M. Di Martino, and E. Dotto 1995. On the evolution of asteroid spin. *Astron. Astrophys.* **299**, 929–932.

Giblin, I., G. Martelli, P. Farinella, P. Paolicchi, M. Di Martino, and P.N. Smith 1998. The Properties of Fragments from Catastrophic Disruption Events. *Icarus* **134**, 77–112.

Gladman, B., P. Michel, Ch. Froeschlé 2000. The Near–Earth object population. *Icarus* **146**, 176–189.

Harris, A.W., 1994. Tumbling asteroids. *Icarus* **107**, 209–211.

Harris, A.W., 2002. On the slow rotation of asteroids. *Icarus* **156**, 184–190.

Kaasalainen, M. et al. 2007. "Acceleration of the rotation of asteroid

1862 Apollo by radiation torques," *Nature* 446: 420-422.

Lowry, S. et al. 2007. "Direct Detection of the Asteroidal YORP Effect," *Science* 316: 272-274.

McInnes, C.R., 1999. *Solar Sailing: Technology, Dynamics and Mission Applications.* Springer-Praxis, Chichester, UK.

Milani, A., Carpino, M., Marzari, F. 1990, Statistics of close approaches between asteroids and planets - Project Spaceguard. *Icarus* **88**, 292–335.

Morrison, D. ed. 1992. The Spaceguard Survey: report of the NASA Near–Earth Object detection workshop (Pasadena: Jet Propulsion Laboratory).

Nesvorný, D. and D. Vokrouhlický. 2007. "Analytic theory of the YORP effect for near-spherical objects," *Astronomical Journal* 134: 1750-1768.

Pravec, P., and Harris, A. W. 2000, Fast and slow rotation of asteroids. *Icarus* **148**, 12–20.

Pravec, P., A.W. Harris, and T. Michalowski 2002. Asteroid rotations. In *Asteroids III*, W.F. Bottke Jr., A. Cellino, P. Paolicchi, and R.P. Binzel Editors. University of Arizona Press, Tucson.

Pravec, P *et al.* 2008. Spin rate distribution of small asteroids *Icarus*, submitted.

Rubincam D.P., 2000, Radiative spin–up and spin–down of small asteroids. *Icarus* **148**, 2–11.

Scheeres, D.J., Marzari, F. and Rossi, A. 2004, Evolution of NEO rotation rates due to close encounters with Earth and Venus, *Icarus* **170**, 312–323.

Scheeres, D.J., Benner, L.A.M., Ostro, S.J., Rossi, A., Marzari, F., Washabaugh, P. 2005, Abrupt alteration of Asteroid 2004 MN4's spin state during its 2029 Earth flyby. *Icarus* **178**, 281–283.

Scheeres, D.J., M. Abe, M. Yoshikawa, R. Nakamura, R.W. Gaskell, P.A. Abell. 2007. "The effect of YORP on Itokawa," *Icarus* 188: 425-429.

Scheeres, D.J.. 2007a. "The dynamical evolution of uniformly rotating asteroids subject to YORP," *Icarus* 188: 430-450.

Scheeres, D.J.. 2007b. "Rotational fission of contact binary asteroids," *Icarus* 189: 370-385.

Scheeres, D.J. and S. Mirrahimi. 2008. "Rotational Dynamics of a Solar System Body Under Solar Radiation Torques," *Celestial Mechanics and Dynamical Astronomy*, in press.

Scheeres, D.J.. 2008. "Minimum energy asteroid reconfigurations and catastrophic disruptions," *Planetary and Space Science*, in press.

Slivan, S. M., Binzel, R. P., Crespo da Silva, L. D., Kaasalainen, M., Lyndaker, M. M., Krco, M. 2003, Spin vectors in the Koronis family: comprehensive results from two independent analyses of 213 rotation lightcurves, *Icarus* **162**, 285–307.

Taylor, P. et al. 2007. "Spin Rate of Asteroid (54509) 2000 PH5 Increasing Due to the YORP Effect," *Science* 316: 274-277.

Vokrouhlický, D., and Capek, D. 2002, YORP–induced long–term evolution of the spin state of small asteroids and meteoroids. I. Rubincam's approximation. *Icarus* **159**, 449–467.

Vokrouhlický, D., S. Breiter, D. Nesvorný and W.F. Bottke. 2007. "Generalized YORP evolution: Onset of tumbling and new asymptotic states," *Icarus* 191(2): 636-650.

Walsh, K.J. and D.C. Richardson. 2008. "A steady-state model of NEA binaries formed by tidal disruption of gravitational aggregates," *Icarus* 193(2): 553-566.

Figure captions

Figure 1. Perihelion distance q evolution of three sample objects in our NEO population, as a function of the evolutionary age. Each line represents the perihelion of a different object.

Figure 2. Distribution of the predicted timescales of the YORP cycles within the simulated population.

Figure 3. Cumulative normalized spin rate distribution of the simulated unbiased (dotted line) and biased population (solid line), compared with the observed NEO observational data (dashed line).

Figure 4. Cumulative normalized spin rate distribution of the unbiased population, simulated with and without YORP effect.

Figure 5. Cumulative normalized spin rate distribution of the unbiased population with different initial spin distribution. The fast rotator population corresponds to our nominal case with initial Maxwellian $\sigma = 2.361$ while the slow rotators have a value of $\sigma = 0.548$, corresponding to an average initial period of 27.46 hr.

Figure 6. Cumulative normalized spin rate distribution of the simulated biased population. The solid line refers to the case where the YORP coefficient C_Y is drawn from a uniform distribution (it is the same as the solid

line in Fig. 3) while the dotted line refers to the case where C_Y is drawn from a Gaussian distribution (with $\sigma = 1.25 \times 10^{-2}$). The distribution of the observed NEO data is plotted for reference too (dashed line).

Figure 7. Cumulative normalized spin rate distribution of the simulated biased population. The solid line refers to the case where only the sign of the YORP coefficient C_Y is changed when reaching the upper limit of the rotation rate (it is the same as the solid line in Fig. 3) while the dotted line refers to the case where both the sign and the absolute value of C_Y are changed when reaching the upper limit of the rotation rate. The distribution of the observed NEO data is plotted for reference too (dashed line).

Figure 8. Cumulative normalized spin rate distribution of the simulated biased population. The solid line refers to the case where the YORP coefficient C_Y is drawn from a uniform distribution and only the sign of the YORP coefficient C_Y is changed when reaching the upper limit of the rotation rate (it is the same as the solid line in Fig. 3). The dotted line refers to the case where C_Y is drawn from a Gaussian distribution (with $\sigma = 0.83 \times 10^{-2}$) and both the sign and the absolute value of C_Y are changed when reaching the upper limit of the rotation rate. The distribution of the observed NEO data is plotted for reference too (dashed line).

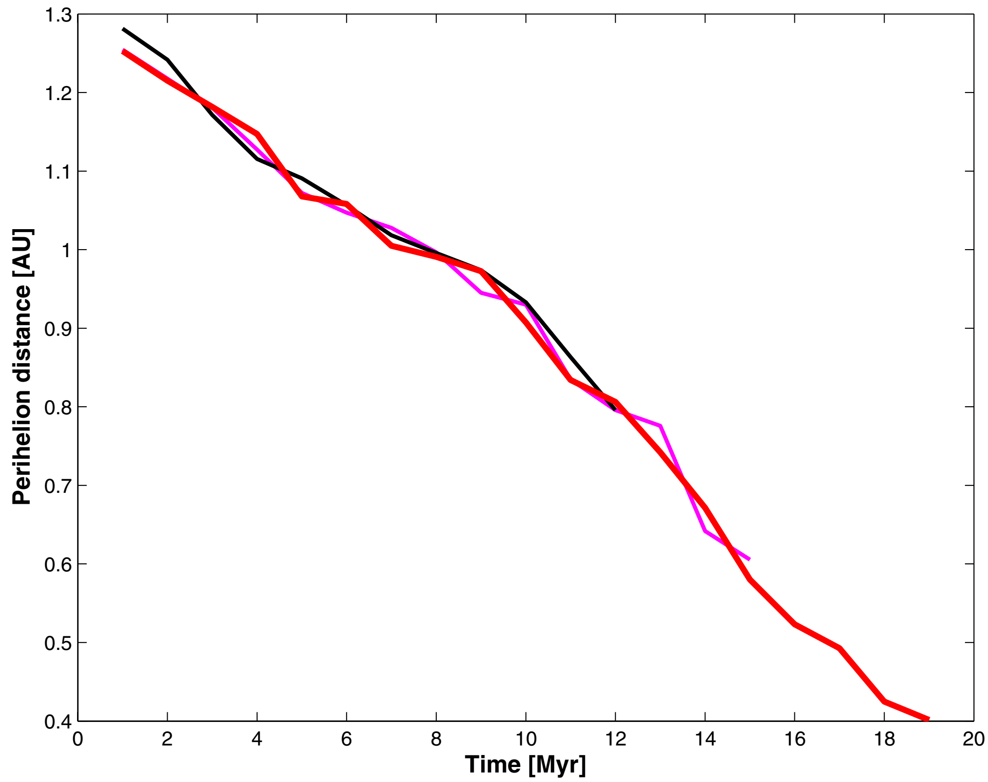

Perihelion distance [AU]
Time [Myr]
1.3
1.2
1.1
1
0.9
0.8
0.7
0.6
0.5
0.4
0
2
4
6
8
10
12
14
16
18
20

Figure 1:

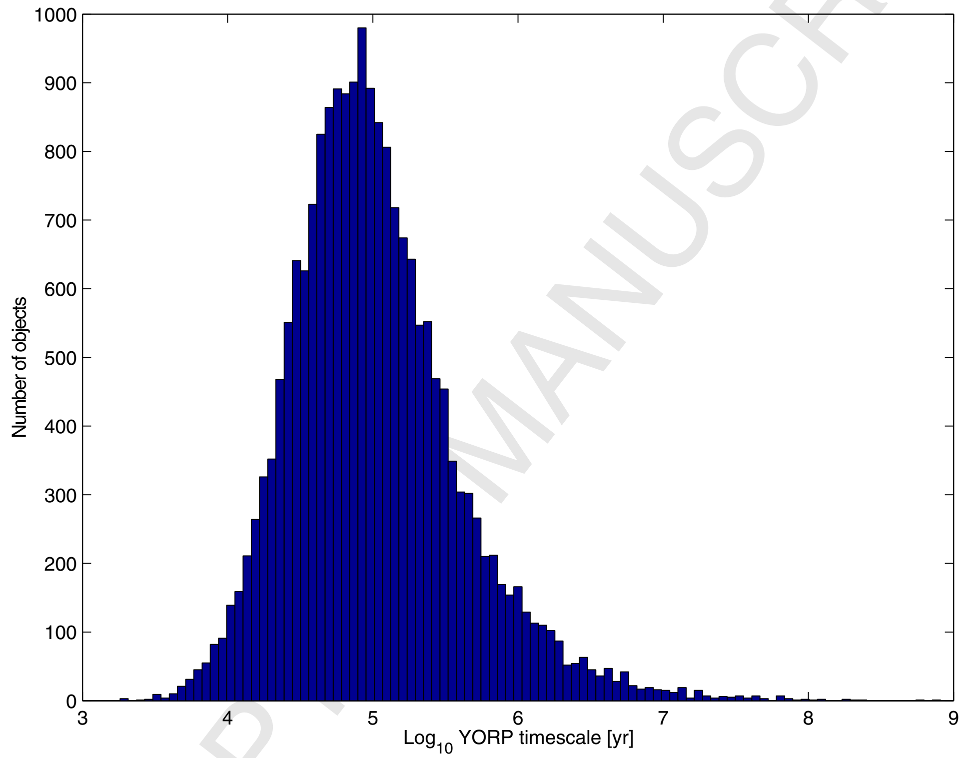

1000
900
800
700
600
500
400
300
200
100
0
Number of objects
3
4
5
6
7
8
9
Log10 YORP timescale [yr]

Figure 2:

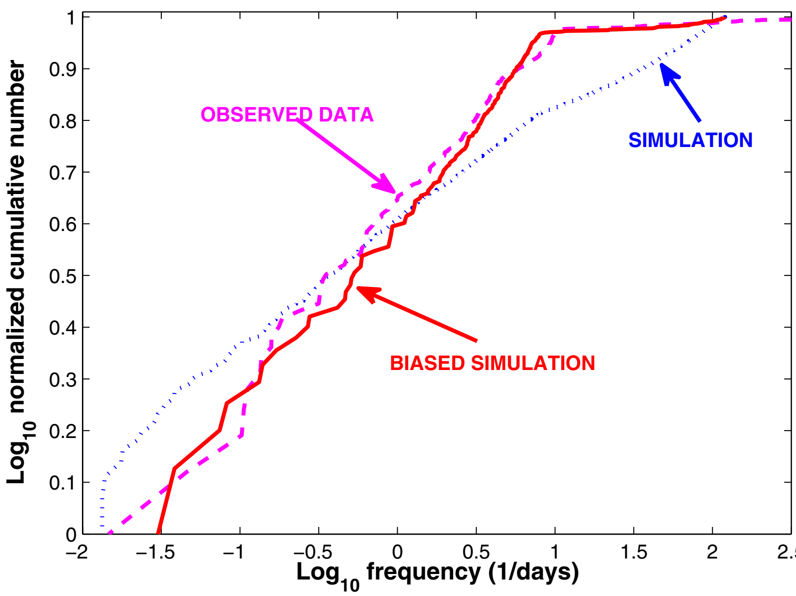
OBSERVED DATA
SIMULATION
BIASED SIMULATION
Log10 normalized cumulative number
Log10 frequency (1/days)
1
0.9
0.8
0.7
0.6
0.5
0.4
0.3
0.2
0.1
0
−2
−1.5
−1
−0.5
0
0.5
1
1.5
2
2.5

Figure 3:

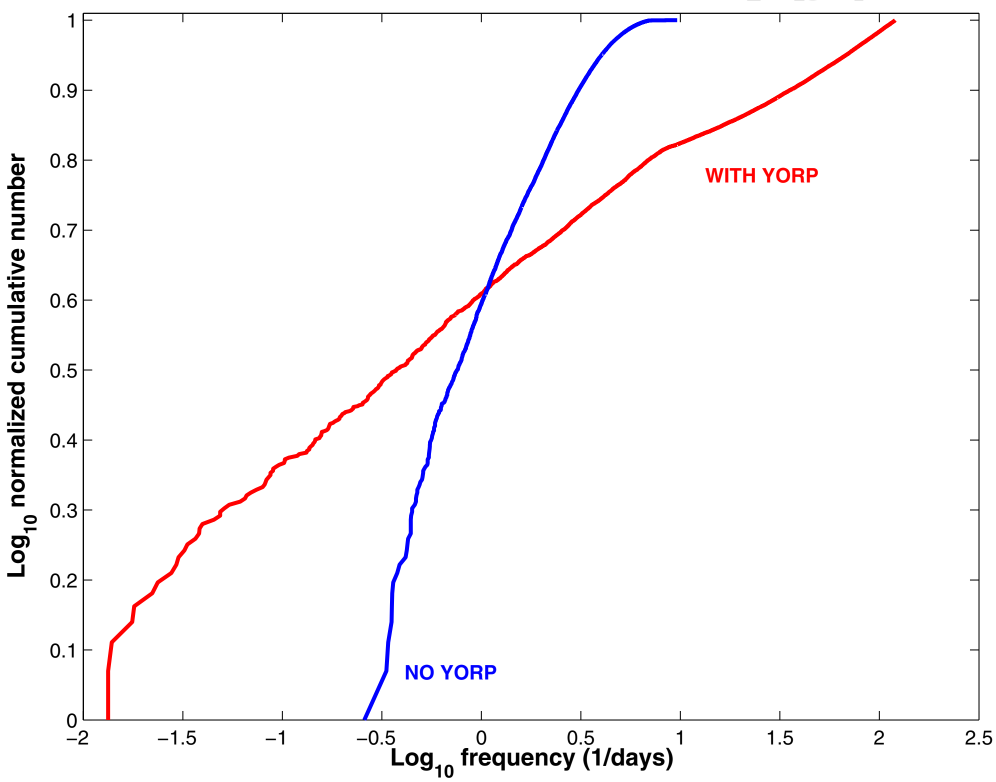

Log10 normalized cumulative number
Log10 frequency (1/days)
WITH YORP
NO YORP
0
0.1
0.2
0.3
0.4
0.5
0.6
0.7
0.8
0.9
1
−2
−1.5
−1
−0.5
0
0.5
1
1.5
2
2.5

Figure 4:

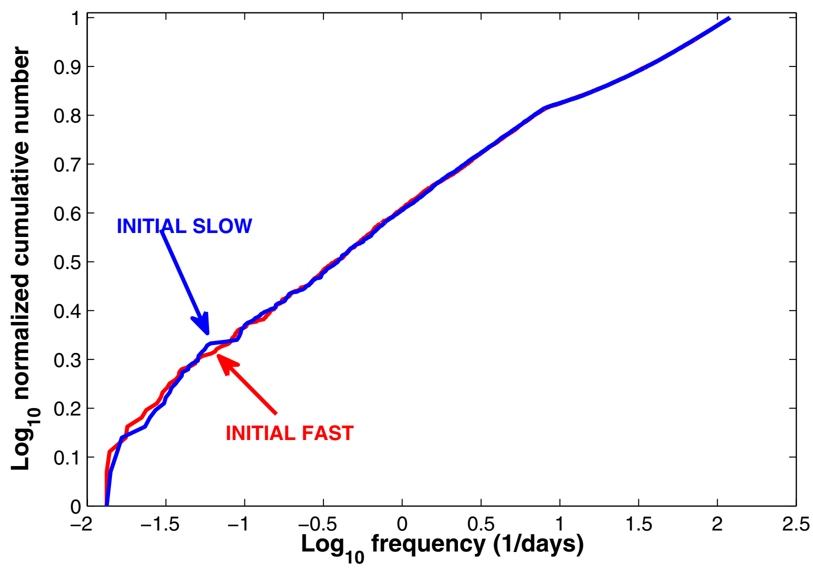

Log10 normalized cumulative number
Log10 frequency (1/days)
INITIAL SLOW
INITIAL FAST

Figure 5:

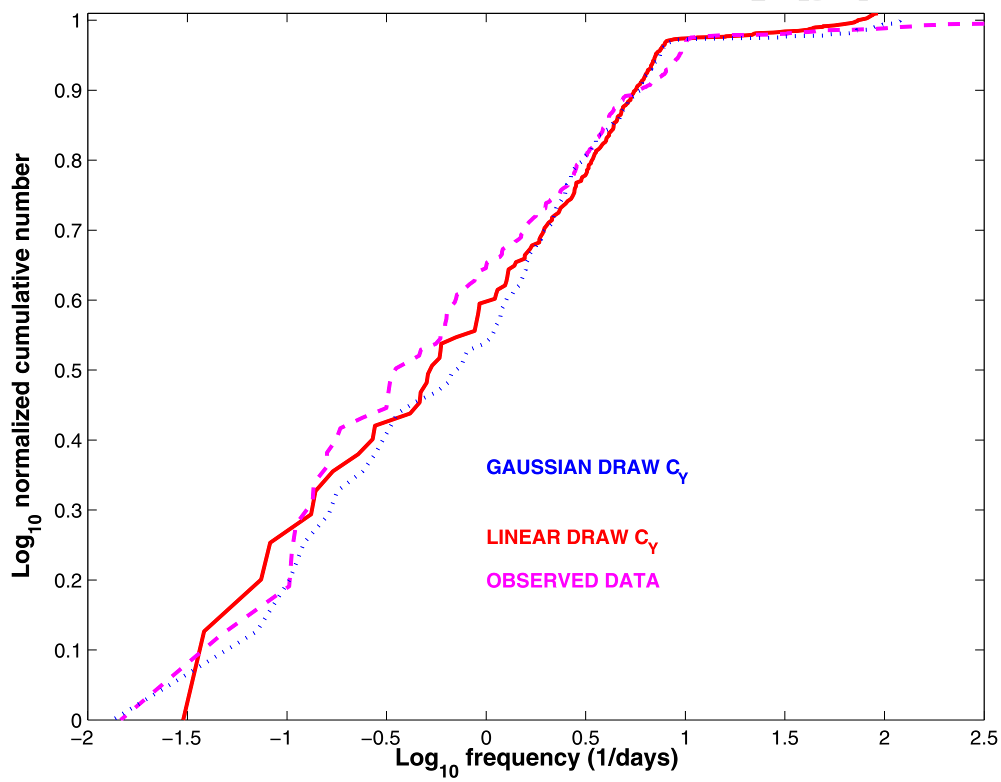

Log10 normalized cumulative number
Log10 frequency (1/days)
GAUSSIAN DRAW CY
LINEAR DRAW CY
OBSERVED DATA

Figure 6:

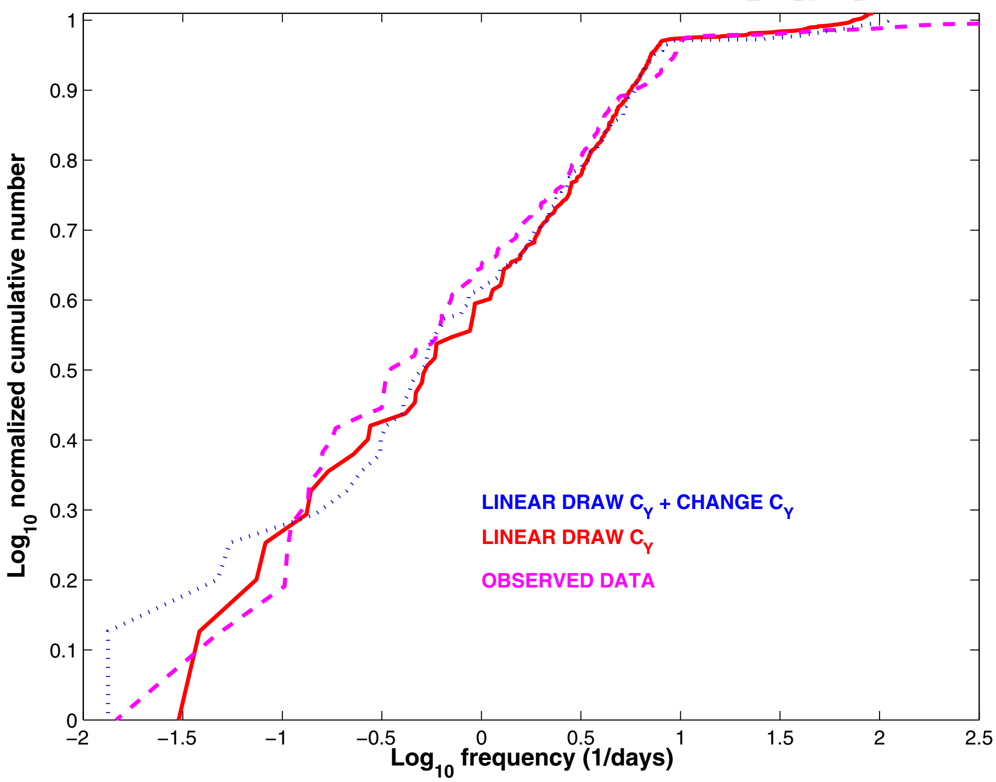

1
0.9
0.8
0.7
0.6
0.5
0.4
0.3
0.2
0.1
0
−2
−1.5
−1
−0.5
0
0.5
1
1.5
2
2.5
Log10 normalized cumulative number
Log10 frequency (1/days)
LINEAR DRAW CY + CHANGE CY
LINEAR DRAW CY
OBSERVED DATA

Figure 7:

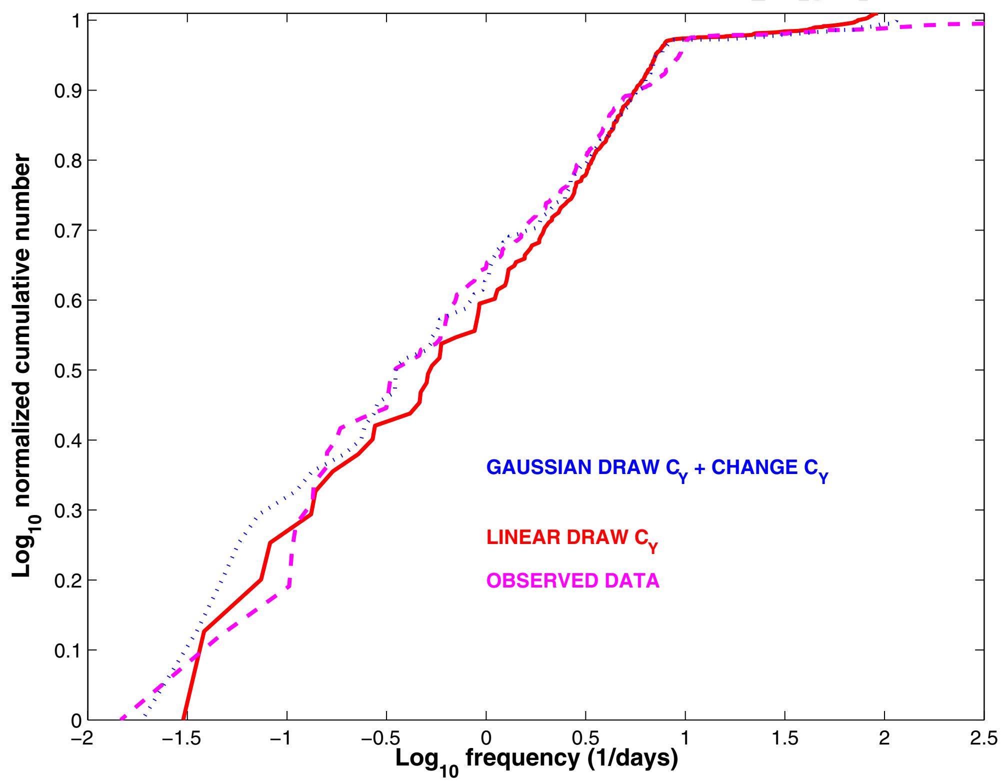

Log10 normalized cumulative number
Log10 frequency (1/days)
GAUSSIAN DRAW CY + CHANGE CY
LINEAR DRAW CY
OBSERVED DATA
0
0.1
0.2
0.3
0.4
0.5
0.6
0.7
0.8
0.9
1
−2
−1.5
−1
−0.5
0
0.5
1
1.5
2
2.5

Figure 8: